ARTICLE TYPE

Dellafossite CuAlO$_2$ film growth and conversion to Cu-Al$_2$O$_3$ metal ceramic composite via control of annealing atmospheres

Daragh Byrne,[1]* Aidan Cowley,[2] Patrick McNally,[2] Enda McGlynn.[1,3]

Daragh Byrne,[1]* Aidan Cowley,[2] Patrick McNally,[2] Enda McGlynn.[1,3]
[1]National Centre for Plasma Science and Technology, Dublin City University, Glasnevin, Dublin 9, Ireland
[2]Nanomaterials Processing Laboratory, Research Institute for Networks & Communications Engineering (RINCE), School of Computing & Electronic Engineering Dublin City University, Glasnevin, Dublin 9, Ireland
10 *[3]School of Physical Sciences, Dublin City University, Glasnevin, Dublin 9, Ireland*
*Author to whom correspondence should be addressed: daragh.byrne2@mail.dcu.ie

In this work we demonstrate simple techniques to form well crystallised CuAlO$_2$ powders and thick films from CuO and boehmite or alumina, using a novel molten salt painting process. We examine the
15 formation mechanism using X-ray diffraction, scanning electron microscopy, energy dispersive X-ray spectroscopy and in situ high temperature X-ray diffraction and find that the annealing atmosphere plays a critical role. From this we develop a method to create Cu-Al$_2$O$_3$ conductive metal-ceramic composite materials with novel morphologies via the thermal decomposition of CuAlO$_2$ precursor films.

1. Introduction

20 There is a growing interest in transparent wide bandgap p-type semiconductor oxides as they may become an essential component in the development of next generation devices in areas such as transparent electronics and solid state UV optoelectronics.[1-3] The discovery of intrinsic wide bandgap p-type
25 conduction in the dellafossite material CuAlO$_2$ represents an important step towards realising these technologies.[4] In addition CuAlO$_2$ as been demonstrated as an effective catalyst for solar water splitting and chlorine production and may also have applications in low power field emission based displays and in
30 sensor technologies.[5-8] Another area, also of increasing interest, is metal ceramic composite (MCC) materials, such as Cu-Al$_2$O$_3$, which have been shown to have favourable properties for many applications, such as high wear resistant conductive coatings, electrodes and structural applications.[9-11]

35 Many different techniques to form CuAlO$_2$ films and powders have been demonstrated including sol-gel, hydrothermal, pulsed laser deposition, MO-CVD and solid state reactions.[12-19] Preparing CuAlO$_2$ using high temperature methods is challenging due to the complex Cu-Al phase diagram.[20] Normally it is
40 considered essential to ensure that the Cu and Al are intimately mixed in order to achieve a phase pure material and this requirement necessitates remixing and multiple anneals when preparing powders using solid state methods. In contrast, by complexing the Cu^{2+} during sol-gel preparation methods phase
45 separation can be inhibited leading to phase pure material, which

can be obtained in a single anneal. Subsequent burn out of the complexing agent leads to a final porous material morphology with many holes in the film.[21] Recently it has been shown that CuAlO$_2$ films with excellent optical properties can be prepared
50 by the interfacial reaction between Cu$_2$O and sapphire substrates using a sandwich structure to inhibit the molten Cu$_x$O from beading on the substrate surface due to surface tension.[22-23] For catalytic applications and for MCCs the use of sapphire is less desirable owing to its high cost and brittleness.

55 In this work we will demonstrate simple techniques for the synthesis of CuAlO$_2$ powders and films on Al$_2$O$_3$ ceramic substrates and their conversion to a MCC, showing the potential CuAlO$_2$ offers in the synthesis of MCCs, e.g. for durable wear resistant conductive ceramics. The initial CuAlO$_2$ film deposition
60 process involves a novel molten salt painting procedure, that with suitable adaption, could be used to coat complex ceramic geometries.

2. Experimental

2.1   Preparation of CuAlO$_2$ reference powder

65 CuAlO$_2$ reference powder was prepared by a solid state reaction between boehmite and CuO. Aluminium isopropoxide was added in small portions to DI-H$_2$O preheated to 80°C under vigorous stirring. CuO powder was then added to the resultant boehmite gel. The molar ratio of Al to Cu was 0.3. The excess water and
70 isopropanol by-product was evaporated from the gel whilst maintaining the vigorous stirring until the viscosity of the gel had

increased to the point where no CuO sedimentation took place. The viscous gel was then transferred to a PTFE dish and heated at 200°C for several hours. During drying an easily handled semi-solid cake formed which was then transferred to a pre-heated furnace at 1100°C for 5 hours. After calcination the cake was quickly removed from the furnace under a nitrogen stream and cooled to room temperature. The excess Cu_xO was then removed by grinding the cake in 36% HCl. The $CuAlO_2$ powder was recovered by vacuum filtration and the filter cake was washed with several aliquots of 36% HCl before being washed with water and then isoproanol and finally dried at 60°C for 24 hours. Excess copper can then be easily recovered from the filtrate.

2.2 Preparation of $CuAlO_2$ films on Al_2O_3

Sintered Al_2O_3 plates 7.5cm x 7.5cm x 1mm were cut into 1 x 2 cm sized samples and cleaned by sonication in acetone and water and gently dried with a nitrogen stream. Copper nitrate was then painted onto the substrate surface in a simple coating procedure. A few crystals of copper nitrate were placed on the surface of the substrate which was then heated to 150°C on a hotplate. When the nitrate salt melted, a small pin was used to paint the entire substrate with the molten salt. After a few minutes heating the molten nitrate lost its water of crystallisation resulting in a dry copper hydroxyl nitrate gel. Over the course of 15 minutes the temperature was increased to 300°C so as to decompose the nitrate, leaving a CuO film on the substrate surface. The coated substrate was then inserted into a pre-heated furnace at 1100°C and heating continued for a further 5 hours to form a $CuAlO_2$ film. The substrates were quickly removed from the furnace under a stream of nitrogen and cooled to room temperature. Excess Cu_xO was removed by soaking the substrate in 36% HCl for 10 minutes, rinsing with fresh HCl, DI-H_2O and dried at 60°C for 1 hour. The entire coating process was then repeated to ensure a uniform and complete coating across the substrate.

2.3 Characterisation and thermal decomposition

The morphologies and crystal structures of the powders and films were examined using scanning electron microscopy (SEM: Karl-Zeiss EVO series) and x-ray diffraction (XRD: Bruker AXS D8 Advance Texture Diffractometer). In situ high temperature XRD measurements and $CuAlO_2$ decompositions were performed using a Jordan Valley D1 Evolution XRD fitted with an Anton Paar DHS1100 domed hot stage.

3. Results

3.1 $CuAlO_2$ powder

$CuAlO_2$ powders prepared by high temperature solid state reactions from mixtures of boehmite gel and CuO showed a good deal of variability in their composition depending on the stoichiometry of reactants used. As shown by the powder XRD data in figure 1(i), samples prepared with a direct 1:1 ratio of [Al] and [Cu] typically had component peaks due to Al_2O_3, indicating an incomplete consumption of the boehmite most likely due to inadequate intermixing of the two reactants. Metallic copper reflections were also detected at 2θ values of 43.3° and 50.4°, corresponding to PDF card no: 04-0836. To eliminate phase impurities, samples are typically re-ground, pressed and re-annealed. In the absence of high pressure pelletisation, re-annealing the as-prepared powders (figure 1 (ii)), leads to a large
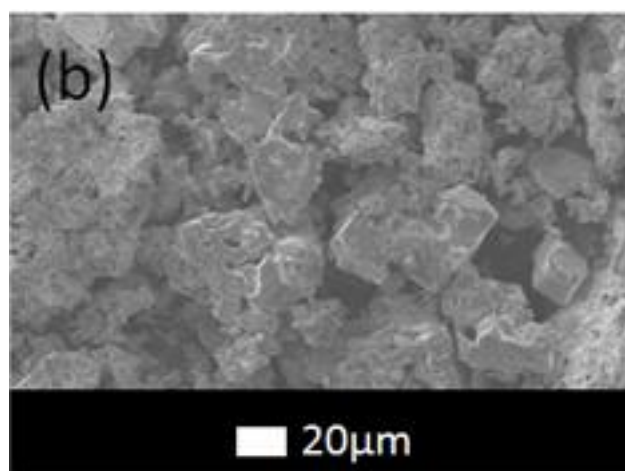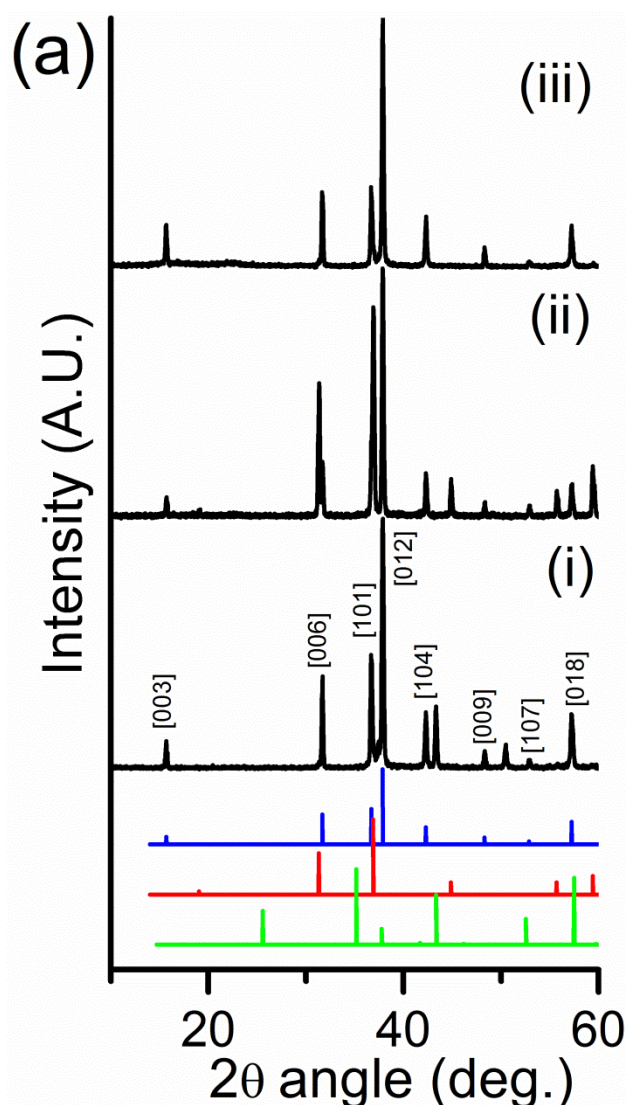

Figure 1: (a) XRD data showing $CuAlO_2$ powder made from boehmite and CuO using [Cu]/[Al] ratios of (i) 1:1 with single anneal at 1100°C (ii) 1:1 with 2 anneals at 1100°C (iii) 3:1 with single 1100°C anneal. The blue, red and green lines indicate the peak positions of $CuAlO_2$ (PDF card no: 35-1401), $CuAl_2O_4$ (PDF card no: 33-0448) and Al_2O_3 (PDF card no: 46-1212), respectively. (b) SEM image showing the $CuAlO_2$ powder corresponding to the XRD data shown in (iii).

increase in the spinel $CuAl_2O_4$ impurity phase as evidenced by the increase of the (220) peak at $2\theta = 31.3°$ and (400) peak at $2\theta = 44.9°$.

As compared to other recent reports using boehmite in conjunction with copper salt precursors where residual impurities remained,[24] it was found that phase pure $CuAlO_2$ powder can be prepared by a single anneal by using an excess of CuO. The XRD data in figure 1 (iii) reveal that, ratios of 3:1 [Cu]/[Al] were sufficient to ensure the complete conversion of the boehmite precursor without the formation of any impurity phases such as residual boehmite or Al_2O_3. Close inspection of the XRD pattern baseline did not reveal any impurity related diffractions indicating that the material is phase pure. The relative intensities of the $CuAlO_2$ peaks identified closely match those of the PDF card 35-1401. The excess copper, which according to the phase diagrams is most likely a mixture of both CuO and Cu_2O, can easily be removed and subsequently recovered by soaking the as-prepared powders in concentrated HCl and filtering.[20] SEM analysis reveal that the phase pure powder is composed of a mixture of morphologies including bulky aggregates of smaller particles along with large well crystallised particles with sizes ranging
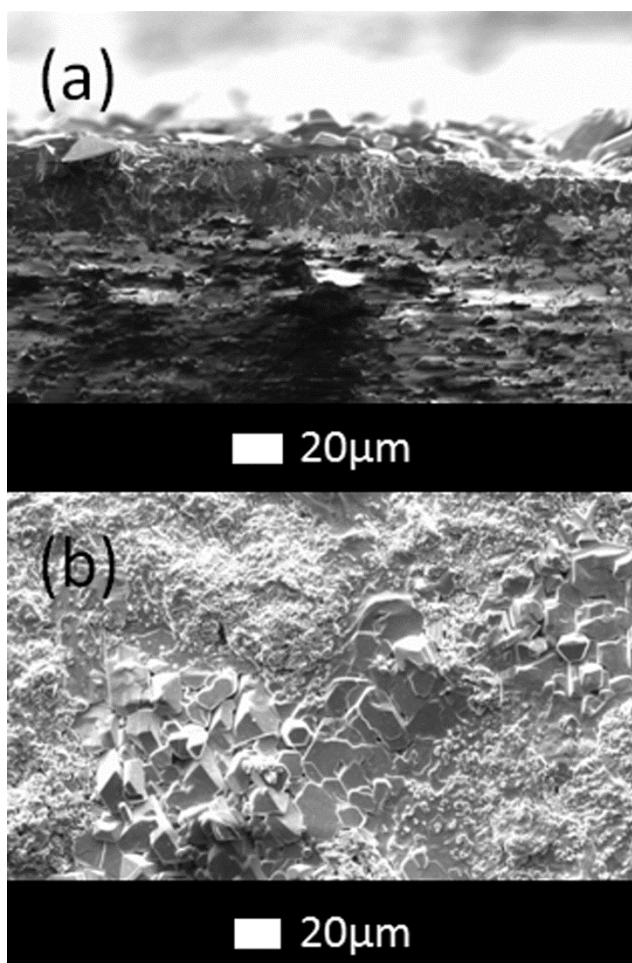
Figure 2: SEM image of (a) cleaved edge and (b) plan view of a $CuAlO_2$ film on Al_2O_3 substrate.

from hundreds of nm up to 40-50µm. Most of the particles are significantly larger than either the CuO or boehmite source powder particles. CuO has previously been used as a flux to grow $CuAlO_2$ single crystals.[18-19] In this case we speculate that the excess CuO may be contributing to the enlarged crystal by acting as a flux, however a number or other explanations are also possible such as the formation of a eutectic or peritectic.

3.2 $CuAlO_2$ Thick films

Thick $CuAlO_2$ films were successfully prepared using the straightforward procedure outlined in the experimental section. The as-prepared films were black in colour and covered the substrates uniformly after two deposition cycles. While many samples had complete substrate coverage after a single deposition cycle, some samples had small gaps in the films where part of the CuO coating dewetted during the annealing step. The SEM images in figure 2 show that the films produced by this technique were typically between 10 and 30µm thick. The thickness range was similar from sample to sample and did not appear to be dependent on the CuO coating thickness.

Similar to the $CuAlO_2$ powders, the films were composed of a variety of particle sizes, ranging from 1-2µm to larger 20-30µm crystals. Cross-sectional SEM analysis reveals that the films vary

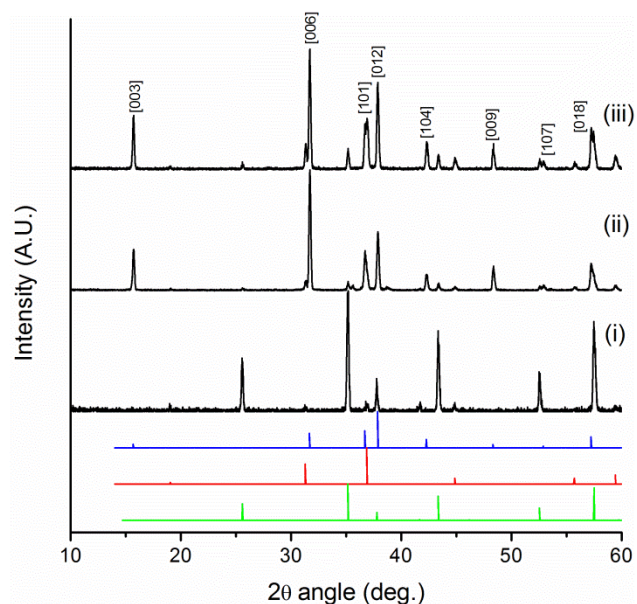Figure 3: XRD data showing (i) the Al_2O_3 substrate (ii) $CuAlO_2$ film made from the interfacial reaction between CuO and Al_2O_3 substrates with 2 deposition cycles (iii) with 2 deposition cycles and a 3rd anneal at 1100°C with the CuO film removed. The blue, red and green lines indicate the peak positions of $CuAlO_2$ (PDF card no: 35-1401), $CuAl_2O_4$ (PDF card no: 33-0448) and Al_2O_3 (PDF card no: 46-1212), respectively.

from being quite dense to slightly porous in some regions. XRD analysis, as shown in figure 3 (ii), indicates that $CuAlO_2$ is the dominant constituent of the film. However, on close inspection, weak diffractions peaks are detected at $2\theta = 31.3°$ and $55.7°$ which are not associated with the substrate (figure 3 (i)) but correspond to spinel impurity phase $CuAl_2O_4$ (220) and (422) planes. After the second deposition cycle, re-annealing the sample as shown in figure 3 (iii), leads to an increase in the impurity spinel phase, which suggests that once formed the spinel

is quite stable and thus difficult to remove. The relative intensity of the $CuAlO_2$ diffraction peaks vary substantially as compared to the reference powder spectra shown in figure 1 (a), implying a texture in the film. Increases are seen in the 2θ peaks located at 15.7° and 31.7° corresponding to the (003) and (006) planes, indicating a preferential growth along the [001] direction.

To further understand the dynamics of the reactions taking place during sintering, CuO and $CuAlO_2$ films on Al_2O_3 were monitored by in situ XRD at 1050°C and 1100°C, respectively. Previously, it has been found that the interfacial reaction between Al_2O_3 and CuO is the origin of the $CuAl_2O_4$ spinel impurity [22-23], whilst earlier studies of the interfacial reaction between CuO, Cu_2O and Al_2O_3 have indicated that $CuAl_2O_4$ preferentially grows on the (0001) plane and $CuAlO_2$ grows on the (11-20).[25] In this work, the polycrystalline Al_2O_3 substrates used have x-ray reflections corresponding to both the (0001) and (11-20) planes and these are used in conjunction with CuO thereby satisfying conditions identified in previous work for both $CuAl_2O_4$ and $CuAlO_2$ formation. However, our results in figure 4 below show that, post annealing, only a very small fraction of the films are in the spinel phase.

It should be noted that the XRD scan range shown in figure 4 and time durations were chosen so as to effectively monitor changes in the sample composition in real time. Each scan lasted 8 minutes and the 2θ range 30 - 40° was chosen as all the components of interest have reasonably strong reflections in this range. At higher temperatures, thermal expansion effects shift the peak positions with respect to room temperature, however the substrate peak provides a useful reference point for the identification of the other components. In addition, peaks remaining at the end of the reaction period were tracked back to room temperature to confirm their assignments. XRD data prior to annealing are shown in figure 4 and curve (i) in figure 4(a) shows reflections at 32.5°, 35.5° and 38.7° corresponding to the (-110) (002) and (111) planes of CuO. The broad FWHM suggest that the dimensions in the crystallographic directions being examined in this region are quite small. SEM images (not shown) of the CuO film prior to annealing, show that the film is composed of CuO nanoblades approximately 100 - 120 nm thick with a cross sectional diameter between 200 and 1000 nm. In the first 8 minutes at 1050°C (curve (ii) of figure 4(a)) the CuO reflections increase in intensity and the peak FHWM decreases. This is most probably due to the sintering behaviour of CuO at high temperature leading to the fusing of smaller grains into larger denser structures and amorphous CuO crystallising.[26] A new weaker peak emerges at 36.3°C which is assigned to the Cu_2O (111) reflection. During the 8-16 minute scan, the CuO peaks completely disappear and are replaced by a dominant Cu_2O peak. After 16 minutes, the Cu_2O film has largely decomposed into metallic copper and alumina (curve (i) of figure 4(c)). In addition to the dominant copper and alumina components a number of weaker diffractions are detected at 2θ = 32.8°, 36.3°, 37.6°, 44.0°, 44.7°, 51.4° and 59.3° which are tentatively ascribed to CuO and $CuAl_2O_4$ and different phases of Al_2O_3. However, the exact origin of these impurities has yet to be determined.

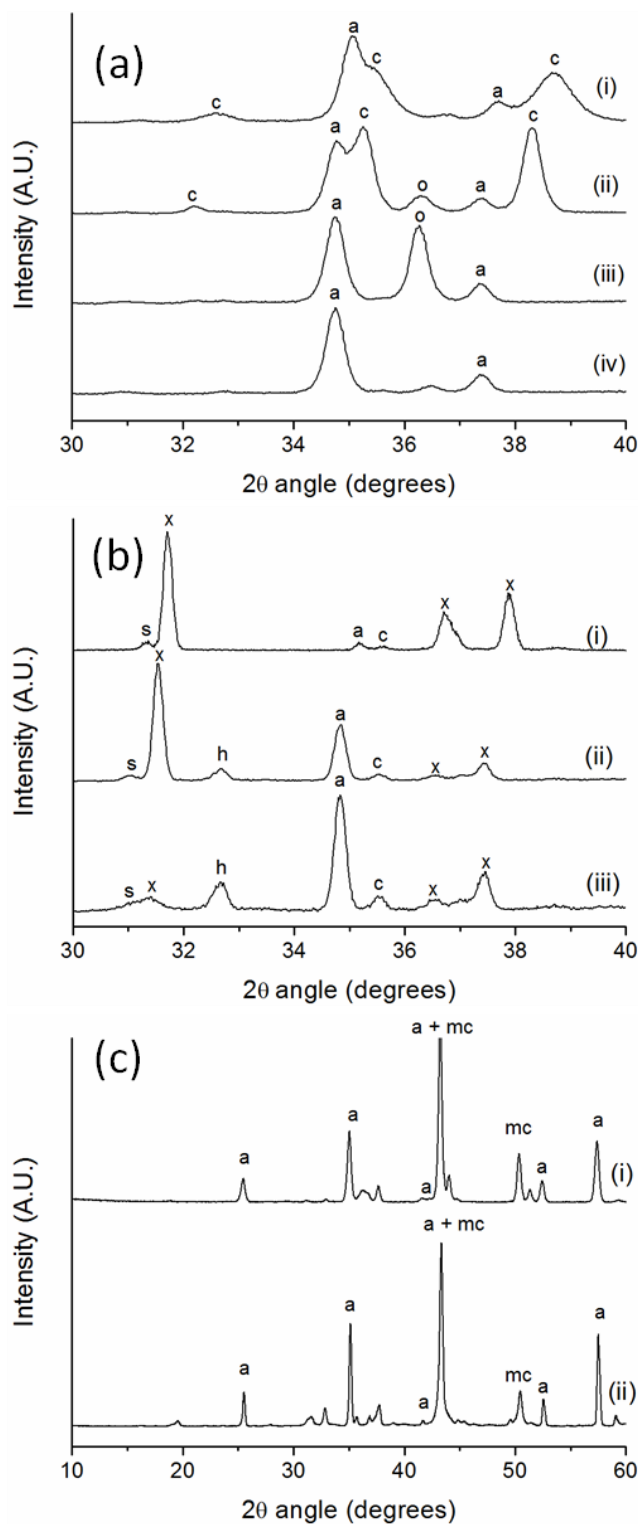Figure 4: XRD data of (a) CuO coated on Al_2O_3 at (i) room temperature (ii) 1050°C,0-8 mins (iii) 1050°C 8-16 mins (iv) 1050°C 16-24 mins. (b) $CuAlO_2$ coated on Al_2O_3 at (i) room temperature (ii) 1100°C 0-8 mins (iii) 1100°C 8-16 mins (c) room temperature diffractogram of (i) CuO coated on Al_2O_3 post annealing at room temperature (ii) $CuAlO_2$ coated on Al_2O_3 post annealing (c = CuO, a = Al_2O_3, o = Cu_2O, mc = metallic copper s = $CuAl_2O_4$, x = $CuAlO_2$ h = AlN heating stage)
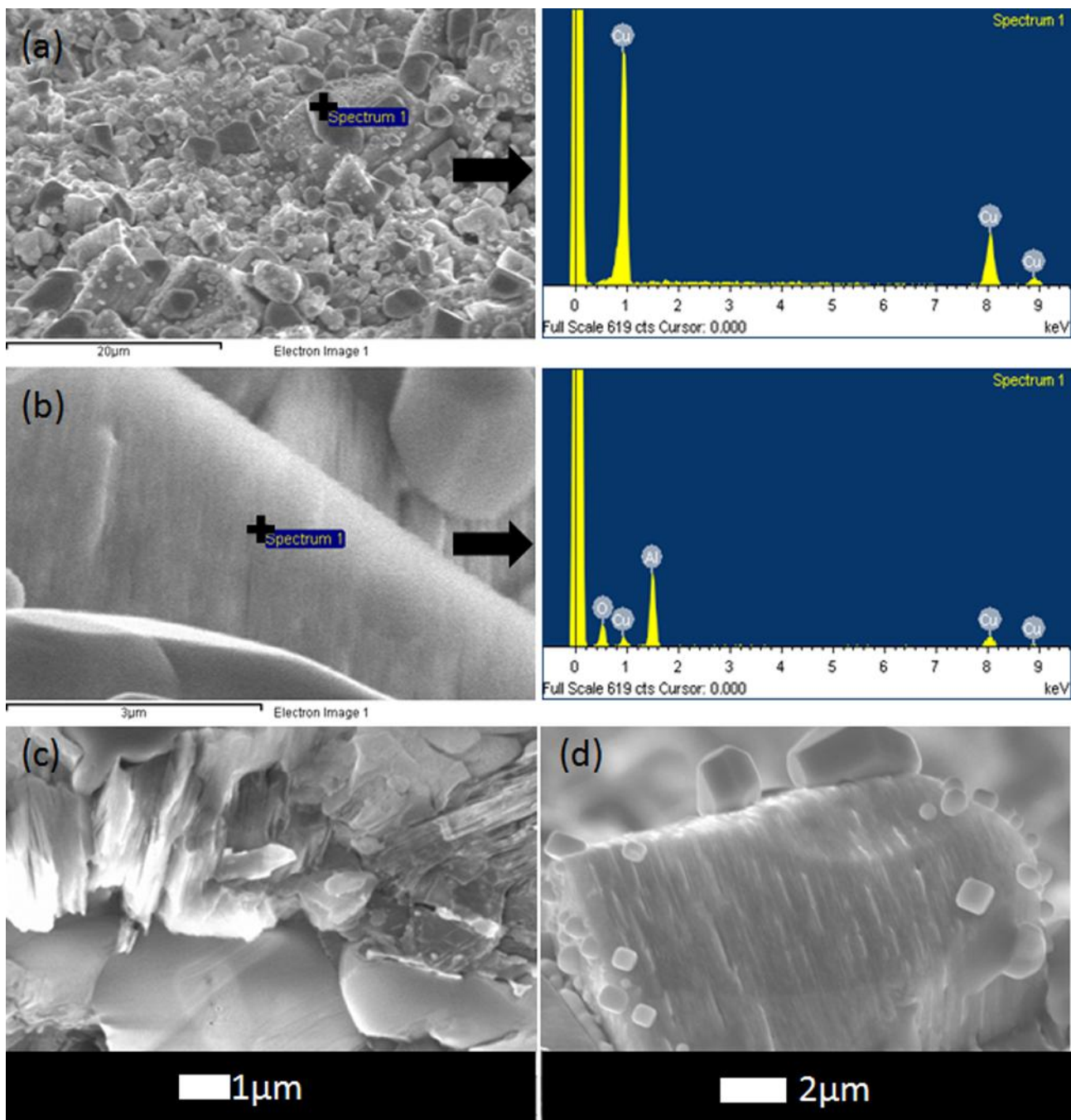
Figure 5: (a) SEM image and EDX spectra of the well faceted discontinuous surface coating. (b) SEM image and EDX spectra of the larger grains of the film coating. (c) and (d) SEM images of the bulk film, highlighting the stratification of the grains.

From these XRD data some interesting points emerge. During this set of experiments, very little copper aluminates were detected, implying the amount formed was very limited (at least at the detection limit of the present measurement). During the initial heating period and during the first 8 minutes when CuO was major component of the film, no $CuAl_2O_4$ was detected, nor was any $CuAlO_2$ detected during the second 8 minutes when Cu_2O was the dominant species present. In addition, the final product formed was metallic copper. The conversion of CuO to Cu_2O at these temperatures is expected as it agrees well with the Cu phase diagrams and other reports.[27-28] During the $CuAlO_2$ film formation excess Cu_2O is clearly evident on the sample surface even after several hours annealing. From this we conclude that the reaction atmosphere plays a critical role in the formation of $CuAlO_2$. The stagnant atmosphere of the heating stage graphite dome inhibits the reaction between the CuO or Cu_2O and Al_2O_3. The gaseous Cu components reduce the oxygen partial pressure sufficiently so as to drive the reaction equilibrium towards the

decomposition of Cu_2O. In an open atmosphere, the Cu vapour can equilibrate with surrounding air, stopping the decomposition process thus allowing the Cu_2O to react with the Al_2O_3, as would be expected by the ternary phase diagram for this system.[20] This suggests that an optimum annealing procedure would consist of two stages with the initial heating being conducted at low oxygen partial pressure so as to encourage the rapid decomposition of CuO, followed by a prolonged anneal at atmospheric oxygen partial pressures so as to enable the reaction between Cu_2O and Al_2O_3. Furthermore, the dependence on annealing atmosphere also suggests that it may be possible to convert previously formed $CuAlO_2$ films to a MCC via a thermal decomposition route. The distinct advantage of this route lies in the fact that the Cu and Al are already intimately mixed at the atomic level, and are of equal stoichiometry, which should yield highly conductive MCCs.

3.3 $Cu-Al_2O_3$ MCC

Figure 4(b) shows the in situ XRD data for a $CuAlO_2$ film annealed at 1100°C. Prior to annealing, the film consisted primarily of $CuAlO_2$, with a small amount of spinel impurity and a trace amount of CuO. The sample was then rapidly heated to the target temperature before scans were commenced. During the first 8 minutes (figure 4(b) curve (ii)), there is a noticeable reduction in the $CuAlO_2$ peak intensities with respect to the substrate peaks. A new peak emerges at $2\theta = 32.6°$, which is identified from room temperature scans as due to the AlN heating stage. Between the 8th and 16th minutes of the anneal, the $CuAlO_2$ film peaks reduced markedly in intensity to the limit of detection. Room temperature XRD post annealing, (figure 4(c) curve (ii)) shows that the sample is now largely composed of Al_2O_3 and metallic Cu, which was confirmed by SEM and EDX analysis as shown in figure 5 (a)-(d). Similar to the CuO annealed samples, a number of weaker additional diffractions were detected at $2\theta = 19.5°, 31.6°, 32.8°, 35.7°, 36.8°, 37.7°, 44.8°$ $45.4°, 49.5°, 51.4°$ and $59.1°$. Given the initial composition of the film prior to annealing, the most likely origin of most of the weaker impurity phases are residual $CuAlO_2$, $CuAl_2O_4$, Al_2O_3 and CuO, which have diffraction peaks in reasonable agreement with those detected.

Post annealing the films are composed of large crystals, with some evidence of faceting, coated by a dusting of smaller well faceted material. EDX analysis of many of these smaller well faceted crystallites indicate that they are composed of reduced metallic copper (figure 5a). The larger grains, which constitute the bulk of the film structure are composed of a composite of Cu and Al_2O_3. EDX analysis of grains free from metallic copper coating (figure 5(b)) confirm the stoichiometry of Cu to Al to O as 1:2:3, matching the expected stoichiometry of a $Cu-Al_2O_3$ MCC. The individual grains of the films appear stratified, being composed of alternating layers, with clear contrast differences in some regions, as shown in the images in figures 5(b) - (d). The alternating crystal structure of the $CuAlO_2$ precursor very possibly plays an important role in the formation of layering. Under these preparation conditions, the $CuAlO_2$ film decomposes, which in turn leads to the reduction of the Cu^{+1} state yielding elemental Cu metal. It is interesting to note that the previously reported phase diagram suggests that $CuAlO_2$ at atmospheric conditions should be stable above 1100°C and 1140°C is the temperature often used to oxidise Cu to form Cu_2O

single crystals.[20,25,29] Experiments performed in open atmospheric conditions confirm the stability of the films up to these temperatures. Therefore a temperature rise or overshoot is unlikely to lead to the decomposition of the $CuAlO_2$ film. Similarly, from the phase diagram it is seen that reducing the temperature range below circa 1000°C at atmospheric conditions decomposes $CuAlO_2$ into $CuAl_2O_4$ and CuO.[20,25] In this work, both CuO films and $CuAlO_2$ films, were observed in situ, reducing to Cu and Cu + Al_2O_3 respectively. It is well known that the composition of Cu_XO melts are dependant on the O_2 partial pressure. At atmospheric oxygen partial pressures, at 1100°C the CuO stability diagram for this system predicts that the final product is Cu_2O with Cu only forming at significantly lower partial pressures.[30] Phase diagram measurements are typically made for bulk materials and therefore the $Cu-Cu_2O-CuO$ system reported in reference 30, may not be direct applicable to this system given that the $CuAlO_2$ is decomposing at an atomic level. At present we are unaware of any reported phase diagrams for the $CuAlO_2$ system at reduced oxygen partial pressures which may explain the anomalous decomposition temperature.

Four point probe electrical measurements in the van der Pauw configuration on these films confirm that they are conductive with a sheet resistance ~1.6 $\Omega/\square$, giving a bulk resistivity of the order of 2-5 mΩcm^{-1}, based on the experimentally determined maximum and minimum film thickness. Given that the phase pure copper identified by EDX on the film surface only forms a discontinuous dusting, it is unlikely to contribute much to the overall film conductivity. Both Cu_2O and CuO are well know p-type semiconductors. The question then arises whether the conductivity is due to the presence of residual oxides or metallic Cu. The lowest reported resistivity for Cu_2O that we are aware of is 12 Ωcm^{-1}, for high quality Si doped single crystals, which is orders of magnitude lower than that of bulk single crystals of CuO.[31,32] Given that our films are polycrystalline and that the resistivity is orders of magnitude lower than that of high quality single crystal Cu_2O, it is also highly unlikely that the conductivity arises from residual oxides. Therefore we speculate that the conductivity arises within the large stratified grains of the material, due to the metallic Cu. However our data are insufficient to comment further at present as to whether the stratifications are linked to the conduction mechanism and the associated issue of the exact distribution of the metallic Cu within the large grains.

4. Conclusions

We have demonstrated that phase pure $CuAlO_2$ powders can be produced in a simple and scalable manner using boehmite and CuO precursors and adjusting the stoichiometry of the starting materials to ensure complete consumption of the boehmite. $CuAlO_2$ films were also produced using a novel molten nitrate salt painting process, the simplicity of which could easily be adapted to coating complex ceramic geometries. To further understand the formation mechanism the reactions of CuO with Al_2O_3 were monitored in situ at high temperature by XRD and this study revealed that the annealing atmosphere plays a critical role in both the formation of $CuAlO_2$ and its spinel impurity phase. Based on this, a method was developed to convert the $CuAlO_2$ into a conductive MCC film with an unusual

(micro/nano) structure via thermal decomposition. Further work is currently underway to examine the tribological and mechanical properties of the MCC films and the possibility of using pressed CuAlO₂ powders to form conductive MCC parts for advanced

5 ceramic applications. Further work is also necessary to clarify the details of the MCC (micro/nano) structure and conduction mechanism.

5. Acknowledgments

References

(1) Banerjee, A. N.; Nandy, S.; Ghosh, C. K.; Chattopadhyay, K. K. *Thin Solid Films* **2007,** *515* (18) 7324-7330

(2) Ling, B.; Sun, X. W.; Zhao, J. L.; Tan, S. T.; Dong, Z. L.; Yang,
20 Y.; Yu, H. Y.; Qi, K. C. *Physica E: Low-dimensional Systems and Nanostructures* **2009,** *41* (4) 635-639

(3) Ling, B.; Zhao, J. L.; Sun, X. W.; Tan, S. T.; Kyaw, A. K. K.; Divayana, Y.; Dong, Z. L. *Applied Physics Letters* **2010,** *97* (1) 013101-013101-013103

25 (4) Kawazoe, H.; Yasukawa, M.; Hyodo, H.; Kurita, M.; Yanagi, H.; Hosono, H. *Nature* **1997,** *389* (6654) 939-942

(5) Mondelli, C.; Amrute, A. P.; Schmidt, T.; Perez-Ramirez, J. *Chem Commun* **2011,** *47* (25) 7173-7175

(6) Smith, J. R.; Van Steenkiste, T. H.; Wang, X.-G. *Phys Rev B* **2009,**
30 *79* (4) 041403

(7) Arghya Narayan, B.; Sang, W. J. *Nanotechnology* **2011,** *22* (36) 365705

(8) Zheng, X. G.; Taniguchi, K.; Takahashi, A.; Liu, Y.; Xu, C. N. *Applied Physics Letters* **2004,** *85* (10) 1728-1729

35 (9) Jamaati, R.; Toroghinejad, M. R. *Materials Science and Engineering: A* **2010,** *527* (27–28) 7430-7435

(10) Shehata, F.; Fathy, A.; Abdelhameed, M.; Moustafa, S. F. *Materials & Design* **2009,** *30* (7) 2756-2762

(11) Fathy, A.; Shehata, F.; Abdelhameed, M.; Elmahdy, M. *Materials &*
40 *Design* **2012,** *36* (0) 100-107

(12) Ding, J.; Sui, Y.; Fu, W.; Yang, H.; Liu, S.; Zeng, Y.; Zhao, W.; Sun, P.; Guo, J.; Chen, H.; Li, M. *Applied Surface Science* **2010,** *256* (21) 6441-6446

(13) Deng, Z.; Zhu, X.; Tao, R.; Dong, W.; Fang, X. *Materials Letters*
45 **2007,** *61* (3) 686-689

(14) Shahriari, D. Y.; Barnabè, A.; Mason, T. O.; Poeppelmeier, K. R. *Inorganic Chemistry* **2001,** *40* (23) 5734-5735

(15) Ingram, B. J.; González, G. B.; Mason, T. O.; Shahriari, D. Y.; Barnabè, A.; Ko, D.; Poeppelmeier, K. R. *Chem Mater* **2004,** *16* (26)
50 5616-5622

(16) Neumann-Spallart, M.; Pai, S. P.; Pinto, R. *Thin Solid Films* **2007,** *515* (24) 8641-8644

(17) Wang, Y.; Gong, H.; Zhu, F.; Liu, L.; Huang, L.; Huan, A. C. H. *Materials Science and Engineering: B* **2001,** *85* (2–3) 131-134

55 (18) Ishiguro, T.; Kitazawa, A.; Mizutani, N.; Kato, M. *Journal of Solid State Chemistry* **1981,** *40* (2) 170-174

(19) Tate, J.; Ju, H. L.; Moon, J. C.; Zakutayev, A.; Richard, A. P.; Russell, J.; Mcintyre, D. H. *Phys Rev B* **2009,** *80* (16)

(20) Jacob, K. T.; Alcock, C. B. *J Am Ceram Soc* **1975,** *58* (5-6) 192-195

60 (21) Jiang, H. F.; Lei, H. C.; Zhu, X. B.; Li, G.; Yang, Z. R.; Song, W. H.; Dai, J. M.; Sun, Y. P.; Fu, Y. K. *Journal of Alloys and Compounds* **2009,** *487* (1–2) 404-408

(22) Shy, J. H.; Tseng, B. H. *Journal of Physics and Chemistry of Solids* **2005,** *66* (11) 2123-2126

65 (23) Shy, J. H.; Tseng, B. H. *Journal of Physics and Chemistry of Solids* **2008,** *69* (2-3) 547-550

(24) Thu, T. V.; Thanh, P. D.; Suekuni, K.; Hai, N. H.; Mott, D.; Koyano, M.; Maenosono, S. *Materials Research Bulletin* **2011,** *46* (11) 1819-1827

70 (25) Susnitzky, D. W.; Carter, C. B. *J Mater Res* **1991,** *6* (9) 1958-1963

(26) Song, J.-H.; Lee, J.-A.; Lee, J.-H.; Heo, Y.-W.; Kim, J.-J. *Ceram Int* (0)

(27) Schramm, L.; Behr, G.; Loser, W.; Wetzig, K. *J Phase Equilib Diff* **2005,** *26* (6) 605-612

75 (28) Fujimura, T.; Tanaka, S.-I. *Acta Materialia* **1998,** *46* (9) 3057-3061

(29) Toth, R. S.; Kilkson, R.; Trivich, D. *Journal of Applied Physics* **1960,** *31* (6) 1117-1121

(30) Neumann, J. P.; Zhong, T.; Chang, Y. A. *Bulletin of Alloy Phase Diagrams* **1984,** *5* (2) 136-140

80 (31) Ishizuka, S.; Kato, S.; Okamoto, Y.; Akimoto, K. *Applied Physics Letters* **2002,** *80* (6) 950-952

(32) Zheng, X. G.; Suzuki, M.; Xu, C. N. *Materials Research Bulletin* **1998,** *33* (4) 605-610